Shin and Kim
Sustainable Environment Research (2024) 34:1
https://doi.org/10.1186/s42834-023-00206-6

Sustainable Environment Research

RESEARCH

Open Access

Hydrothermal synthesis of zeolites from residual waste generated via indirect carbonation of coal fly ash

Seonmi Shin[1,2] and Myoung-Jin Kim[1,2*]

Abstract

Indirect carbonation, a technology to store CO_2 and produce stable $CaCO_3$ and $MgCO_3$, involves elution of Ca and Mg from industrial waste and subsequent carbonation. Although substantial residual waste is generated after the elution of Ca and Mg, its recycling attributes have not been adequately scrutinized. The residual waste has lower Ca and Mg contents and higher Si and Al contents than those of the raw material (i.e., industrial waste). This study involves the hydrothermal synthesis of zeolite-P using residual waste from indirect carbonation, conducted at both 100 and 180 ℃. The properties of these zeolites are compared with those synthesized from coal fly ash (CFA). The synthesized zeolites were characterized by X-ray diffraction, field emission scanning electron microscope, thermogravimetric analyzer, and Brunauer–Emmett–Teller (BET). A high zeolite conversion efficiency was achieved through a hydrothermal reaction (up to 87%), even though Si and Al were not added to the residual waste. Additionally, the cation exchange capacity and BET specific surface area of the synthesized zeolites were high (200 cmol kg^{-1} and 73 m^2 g^{-1}, respectively). These findings highlight the possibility of synthesizing zeolites using the residual waste from indirect carbonation as an alternative to conventional zeolite synthesis using industrial waste such as CFA. The synthesized zeolite-P is expected to be effective in wastewater treatment, detergent manufacturing, and water softening.

Keywords Zeolite, Residual waste, Indirect carbonation, Hydrothermal synthesis, Coal fly ash

1 Introduction

Zeolites have a three-dimensional structure comprising Al, O, Si, other alkali metals (Na and K), and H_2O molecules [1]. They are porous materials with a large surface area and have cavities arranged in an aluminosilicate hydrate framework with a negative charge. Over the past few decades, the demand for zeolites has significantly increased owing to their emerging applications in various fields including catalysis, adsorption, water softening, wastewater treatment, and agriculture. Approximately 150 different synthetic zeolites are currently synthesized worldwide, which account for a total annual zeolite production of approximately 3 Mt [2]. The global zeolite market, which was valued at USD 4326 million in 2019, has been projected to be worth USD 6190 million in 2027 [2]. However, significant challenges such as the production cost of synthetic zeolites and logistical constraints exist in this arena [2, 3]. Commercially, zeolites are produced from chemical precursors such as $NaAlO_2$ and Na_2SiO_3, making them considerably expensive. Therefore, alternative zeolite synthesis routes featuring reliable and economical source materials such as coal fly ash (CFA) [1, 4], red mud [5], and kaolin [6, 7] have been studied. The synthesis of zeolites using industrial waste

*Correspondence:
Myoung-Jin Kim
kimmj@kmou.ac.kr
[1] Department of Environmental Engineering, Korea Maritime and Ocean University, Busan 49112, Republic of Korea
[2] Interdisciplinary Major of Ocean Renewable Energy Engineering, Korea Maritime and Ocean University, Busan 49112, Republic of Korea

containing abundant Si and Al instead of pure chemical reagents can assist in improving economic efficiency and reducing environmental pollution.

In this study, experiments were conducted to synthesize zeolites using the residual waste obtained via indirect carbonation of CFA—a coal combustion waste. Indirect carbonation is a technology for producing stable $CaCO_3$ and $MgCO_3$, which involves extracting Ca and Mg from industrial waste or natural minerals using solvents, such as acids and ammonium salts, and then reacting them with CO_2 [6–8]. Although indirect carbonation shows promise as a carbon–neutral technology for CO_2 storage, it is disadvantageous in terms of its questionable economic feasibility and landfill utilization for residual waste. Substantial residual waste is generated after the solvent-based extraction of Ca and Mg from industrial waste. Valuable components of the residual waste (i.e., Si and Al), which are present in industrial waste, remain intact but are landfilled. Notably, although the Ca and Mg contents of the residual waste are low, the contents of valuable elements such as Si and Al are often high. To the best of our knowledge, few studies have been conducted to date on recycling the residual waste from indirect carbonation.

CFA has previously been used as a material for indirect carbonation owing to its high Ca content as well as zeolite synthesis because of its high Si and Al contents [2, 9–12]. CFA is a highly abundant industrial solid waste used for zeolite synthesis. Moreover, it is an excellent waste material for synthesizing meso- and microporous materials because of its similar chemical composition and physicochemical properties to those of zeolite [2, 9, 10]. Although zeolite and CFA have similar elemental compositions, they differ in terms of their crystalline structure.

In terms of chemical composition, CFA primarily contains silica, alumina, ferrous oxide, and calcium oxide, along with different amounts of residual carbon and trace elements. However, significant inter- and intra-regional differences exist with respect to the composition [13]. The chemical composition of CFA varies with location, the type of coal burned, burning conditions, and the origin of the parent coal. The composition and mineralogical phase content of CFA are principally influenced by the origin and type of coal burned in power plants. Generally, the CFA derived from sub-bituminous and lignite coals is characterized by higher CaO, MgO, and SO_3 contents and lower SiO_2 and Al_2O_3 amounts than those of higher-grade fuels such as bituminous and anthracite coals [14].

The hydrothermal technique is considered the primary route for synthesizing zeolites using CFA. In this technique, water and a base are used as a solvent and mineralizer, respectively, at various temperatures and pressures. Zeolites are frequently synthesized using the hydrothermal approach owing to its advantages such as low energy consumption, high reactant reactivity, straightforward maintenance of the solution, low air pollution, and formation of metastable phases and unique condensed phases [13]. In hydrothermal treatment, the amount of aluminate or silicate is typically varied to obtain a desired type of zeolite. Different synthetic zeolites such as zeolite X, zeolite P, zeolite A, analcime, chabazite, and hydroxyl sodalite can be produced by altering reaction conditions such as temperature (80–200 C), reaction time (2–48 h), Si/Al ratio (1–15), alkaline solution concentration, pH, and seeding of initial CFA [15, 16].

In this study, we synthesized crystalline zeolite-P through a hydrothermal reaction using the residual waste produced after indirect carbonation to improve the economic feasibility of indirect carbonation technology and to implement a zero-discharge system. Zeolites were synthesized via the hydrothermal reaction of CFA-derived residual waste at low and high temperatures (100 and 180 C), and their properties were compared with those of zeolites obtained via the hydrothermal reaction of CFA. Additionally, the conversion efficiencies of the synthesized zeolites were determined by comparing the dehydration weight loss of synthesized zeolite and pure zeolite [15].

2 Materials and methods

2.1 Materials

CFA obtained from a thermal power plant in Korea was used as an indirect carbonation material. The CFA particles were ≤ 425 μm in size. The following analytical-grade chemicals were used in the experiments: ammonium chloride (98.5%), hydrochloric acid (36.0%), and sodium hydroxide (97.0%). X-ray diffraction (XRD; SmartLab, Rigaku, Japan) and X-ray fluorescence (XRF; XRF-1700, Shimadzu, Japan) analyses were conducted to determine the components and properties of solid samples. Field emission scanning electron microscopy (FE-SEM; MIRA-3, Tescan, Czech Republic) and thermogravimetric analysis (TGA; TGA 7, Perkin Elmer, USA) were performed to examine the surface morphology of the solids and determine the temperature-dependent weight loss, respectively. For the TGA, each sample was placed on a Pt plate and heated from 50 to 900 C at 20°C min^{-1} to measure its weight change. The specific surface area of the solids was measured using the Brunauer–Emmett–Teller (BET) method (Autosorb-iQ, Quantachrome, USA).

2.2 Experimental methods

2.2.1 Zeolite synthesis using residual waste

First, the residual waste from indirect carbonation was prepared as a raw material to synthesize zeolites.

CFA and an indirect carbonation solvent (0.3 M HCl or 0.3 M NH_4Cl) were mixed at a ratio of 1:50 (g:mL) and stirred at 250 rpm for 1 h. The solvents have been commonly used in previous studies on indirect carbonation [8–10, 16–20]. The solids obtained by filtering the resulting suspension were dried. The products obtained using HCl and NH_4Cl—referred to as 'residual waste' herein—are denoted as RW-HCl and RW-NH_4Cl, respectively.

The zeolite synthesis is described henceforth. The two residual waste specimens were separately mixed with a 2 M NaOH solution at a ratio of 1:5 (g:mL) and then aged by stirring at 250 rpm at room temperature for 4 h. The resulting suspensions were hydrothermally reacted at 100 C for 24 h while stirring at 250 rpm and then filtered. The obtained solids were dried at 90 C for 12 h. The hydrothermal synthesis was also performed at 180 C. Additionally, zeolites were hydrothermally synthesized using CFA at 100 and 180 ℃ in the same manner. The synthesized zeolites—denoted as ZE-CFA-100, ZE-HCl-100, ZE-NH_4Cl-100, ZE-CFA-180, ZE-HCl-180, and ZE-NH_4Cl-180— were analyzed by XRD, XRF, TGA, and FE-SEM.

2.3 Adsorption properties of the synthesized zeolites

The cation-exchange capacity (CEC) and BET specific surface area were measured to evaluate the adsorption capacity of the zeolites hydrothermally synthesized at 100 and 180 C, and these values were compared with those of the raw materials (RW-NH_4Cl, RW-HCl, and CFA). The CEC was determined using the ammonium method (EPA test method 9081).

3 Results and discussion

3.1 Zeolite synthesis using residual waste

The Si and Al contents of the CFA were 58 and 18%, respectively, which were considerably higher than those of the other components; the Si/Al ratio was 3.2. The Si and Al contents of the residual waste were 58–60% and 21–24%, respectively, which were higher than those of the CFA; the Si/Al ratio was 2.3–2.8. The Si/Al ratios of both the CFA and residual waste were appropriate; therefore, additional aluminum or silicate was not required to synthesize zeolite P [19–21].

XRD analysis indicated that the primary components of both the residual waste and CFA were quartz (SiO_2) and mullite [$3(Al_2O_3)\cdot 2(SiO_2)$] (Fig. 1a–c), which are

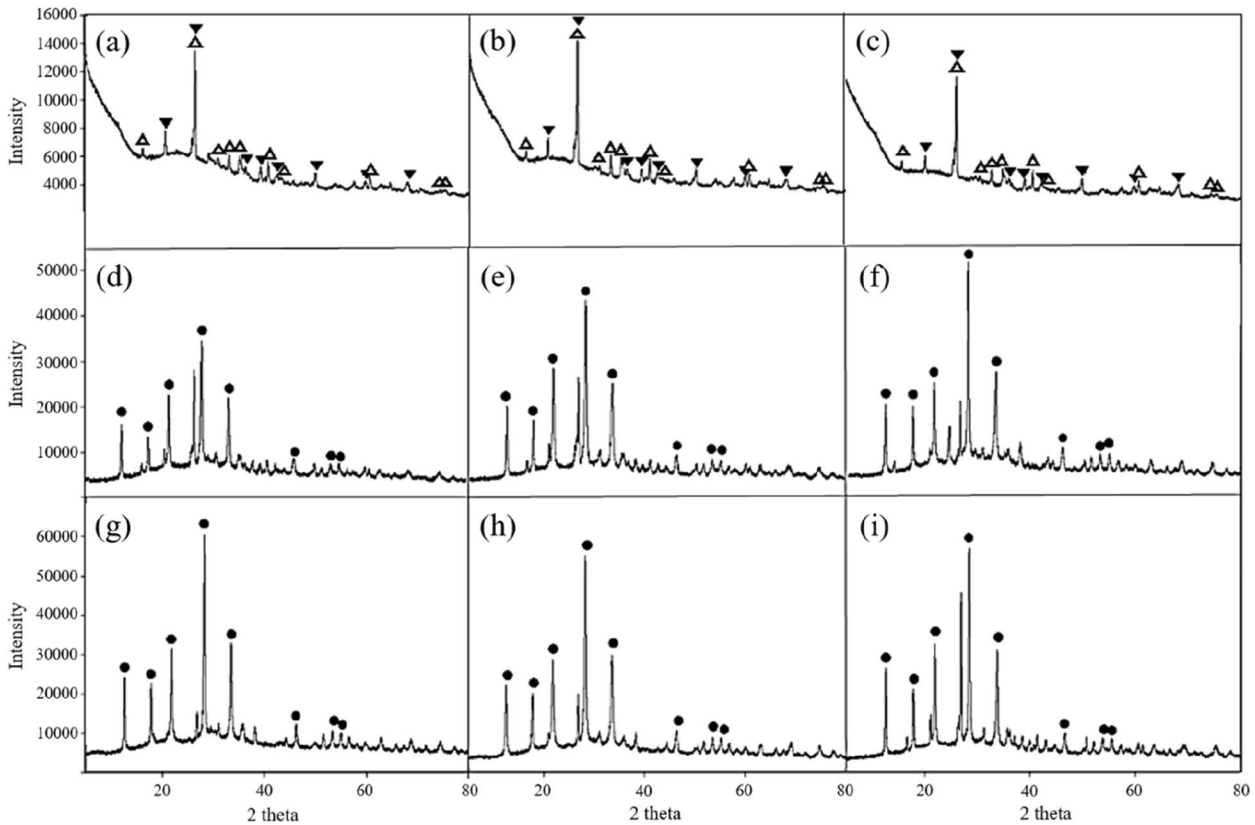

Fig. 1 XRD patterns of raw materials and synthesized zeolites: **a** CFA, **b** RW-HCl, **c** RW-NH_4Cl, **d** ZE-CFA-100, **e** ZE-HCl-100, (f) ZE-NH_4Cl-100, **g** ZE-CFA-180, **h** ZE-HCl-180, and **i** ZE-NH_4Cl-180. (△: quartz, ▼: mullite, ●: zeolite P)

precursors of hydrothermally synthesized zeolites and can act as sources of Si and Al, respectively. FE-SEM images of the residual waste and CFA revealed their spherical shape and smooth surfaces that hardly had any pores (Fig. 2a–c).

The solids obtained via hydrothermal synthesis at 100 and 180 C were confirmed to be zeolite P through their XRD patterns (Fig. 1d–i). P-type zeolites are known to belong to the gismondine family and exhibit unique characteristics [13]. In particular, zeolite P can be used for wastewater treatment and agriculture. To construct the zeolite structure during the hydrothermal process, the Si and Al components of the residual waste and CFA must be dissolved in a solution first; the aging process plays a vital role in this regard [22]. During the aging process conducted for more than 4 h in the present study, the Si and Al from quartz and mullite were dissolved in NaOH solution to form water-soluble sodium aluminosilicate. As a result, the aging conducted in the alkaline solution prior to the hydrothermal reaction promoted the zeolite synthesis [23, 24].

The XRD peak intensities of the zeolites synthesized at 180 C (54,000–60,000 counts; Fig. 1g–i) were approximately 1.5 times higher than those of the zeolites synthesized at 100 C (34,000–53,000 counts; Fig. 1d–f). The overall crystallinity and content of synthetic zeolites increase with increasing hydrothermal temperature [25]. The differences between the zeolites formed at different temperatures can be ascribed to the properties of mullite—a mixture of silicon and aluminum oxide—which is more stable than quartz—a silicon oxide. Because of the low solubility and inertness of mullite, the zeolite formation could be limited depending on the synthesis conditions [14]. In other words, the hydrothermal synthesis of zeolites using residual waste and CFA could have disadvantages such as the partial dissolution of Si and a lower dissolution rate of Al than that of Si at 100 C.

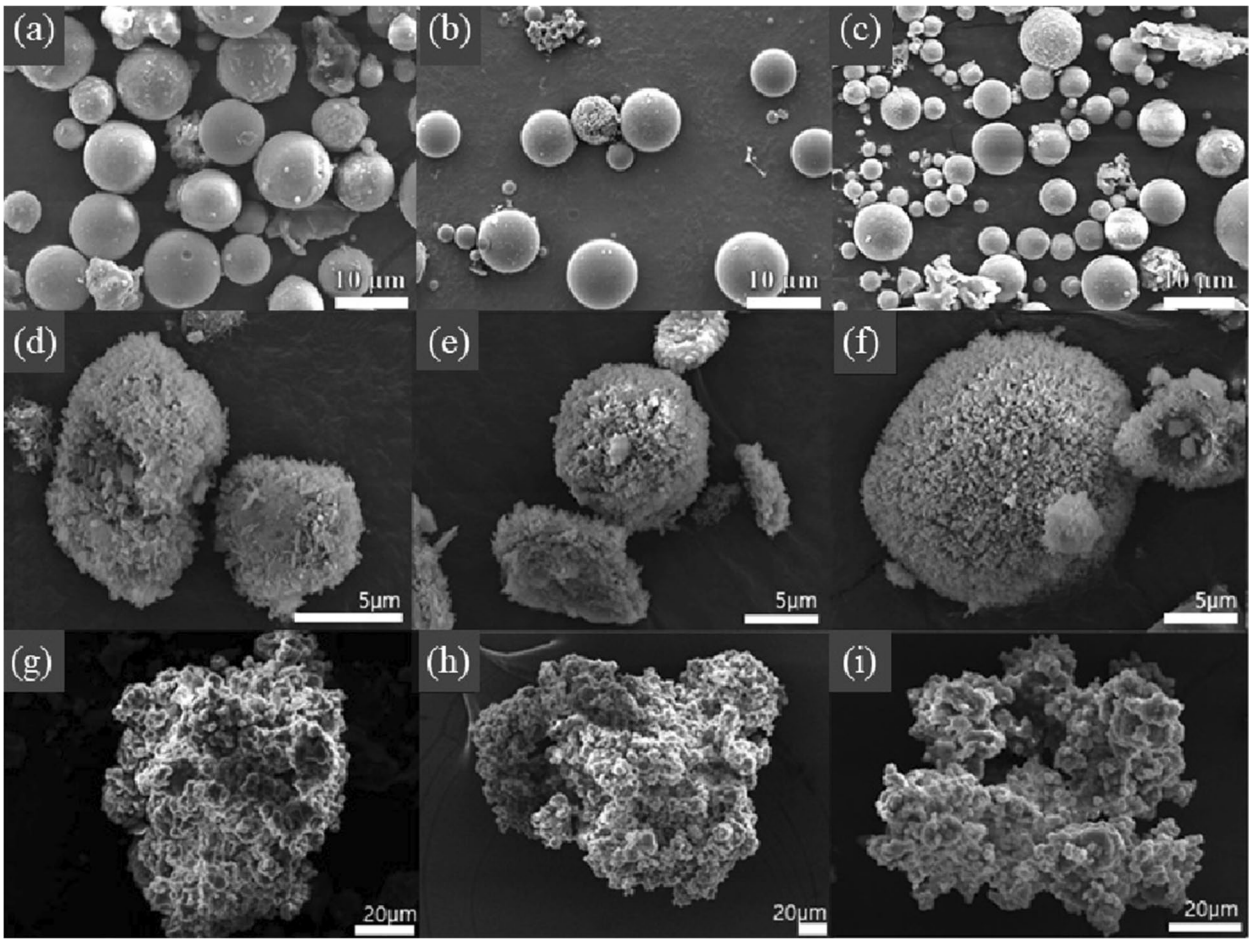

Fig. 2 FE-SEM images of raw materials and synthesized zeolites: **a** CFA, **b** RW-HCl, **c** RW-NH_4Cl, **d** ZE-CFA-100, **e** ZE-HCl-100, **f** ZE-NH_4Cl-100, **g** ZE-CFA-180, **h** ZE-HCl-180, and **i** ZE-NH_4Cl-180

FE-SEM images of the synthesized zeolites (Fig. 2d–i) revealed a significantly higher number of pores in the synthesized zeolites than those in the raw materials (i.e., the residual waste and CFA). The zeolites hydrothermally synthesized at 100 C had a cactus-like spherical shape with many flat parts on their surfaces (Fig. 2d–f). In contrast, the zeolites synthesized at 180 C were irregularly shaped and had a coral-like morphology with extremely rough surfaces (Fig. 2g–i). Notably, the zeolites synthesized at 180 C had larger surface areas than those of the zeolites synthesized at 100 C. Depending on the SiO_2/Al_2O_3 ratio and other synthesis conditions, zeolite P exhibits different morphologies such as cylindrical, rectangular-prism-shaped, donut-like, fiber-like, diamond-like, cactus-like, nut-like, cabbage-like, and wool-ball-like morphologies [20].

Table 1 lists the XRF results of the zeolites hydrothermally synthesized at 180 C. Compared to the Na_2O contents of the raw materials (0.98–1.13%), those of the synthesized zeolites increased significantly to 9.8–11.5%. The molecular formula of the synthesized zeolite-P calculated using the XRF results was $Na_6Al_{6.9-7.9}Si_{12.3-16.9}$, whose Na:Al:Si molar ratio is relatively close to that of the theoretical formula ($Na_6Al_6Si_{10}O_{32}$•$12H_2O$; identified by XRD) [20]. Impurities other than the zeolites possibly existed in the hydrothermally synthesized solids because the suspension (raw materials and NaOH solution) was hydrothermalized without removing any impurities after the suspension was aged.

The Si/Al ratio of zeolites influences their adsorption properties. Low-silica zeolites (Si/Al < 2) have high ion-exchange capacity and can be used to adsorb ammonium and heavy metals [2, 26]. This is applicable to the zeolites synthesized using residual waste at 180 C in this study, as their Si/Al ratio was 1.8–1.9 (Table 1). Note that the Si/Al ratio of the zeolites synthesized using residual waste is lower than that of ZE-CFA-180 and seemingly within the desirable limit, indicating superior applicability.

3.2 Zeolite conversion efficiency

Figure 3 shows the TGA results of the six zeolites synthesized using the residual waste and CFA and that of pure zeolite-P synthesized using Na_2SiO_3 and $NaAlO_2$ [27]. The TGA results were used to calculate the conversion efficiencies of the six zeolites. According to [15], the conversion efficiency of synthesized zeolites can be reliably calculated by TGA compared to other analytical methods. When a zeolite is heated, weight loss occurs owing to moisture loss at 40–400 C. Specifically, the loss of physically adsorbed moisture present in the zeolite pores occurs at 40–200 C, and the loss of moisture in the hydration complex formed using exchangeable cations occurs at 200–400°C [28]. In the temperature range 40–400 C, the zeolites hydrothermally synthesized at 100 and 180 C exhibited weight losses of 12.0–15.5% and 16.0–16.5%, respectively; pure zeolite-P showed a weight loss of 18.5% (Table S1).

Table 1 Molecular formulae of the synthesized zeolites calculated using the XRF results

Synthesized zeolite	Weight (%)			Molecular formula	Si/Al ratio
	SiO_2	Al_2O_3	Na_2O		
ZE-CFA-180	54	21	10	$Na_6Al_{7.9}Si_{16.9}$	2.1
ZE-HCl-180	49	24	12	$Na_6Al_{6.9}Si_{12.3}$	1.8
ZE-NH_4Cl-180	49	22	12	$Na_6Al_{7.1}Si_{13.3}$	1.9

The conversion efficiency (%) was calculated by dividing the weight loss of the synthesized zeolite by that of pure zeolite P and multiplying by 100. The conversion efficiencies of the zeolites hydrothermally synthesized at 100 and 180 C were 65–84% and 87–89%, respectively; essentially, the zeolites exhibited a higher conversion efficiency at higher hydrothermal temperatures (Table 2). Notably, the zeolites hydrothermally synthesized at 180 C using only the residual waste and CFA without additional Si and Al exhibited high conversion efficiencies of up to 89%, with little difference observed in the zeolite conversion efficiency between the residual waste and CFA. These results suggest that both the residual waste from indirect carbonation as well as CFA, which has been extensively used to synthesize zeolites can be used to synthesize high-performance zeolites.

3.3 Adsorption properties of zeolites

Table 3 lists the CECs of the raw materials and synthesized zeolites. The CECs of the residual waste and CFA were similar and considerably low (4.8–5.3 cmol kg^{-1}). These values are similar to those of previously investigated CFA [29, 30]. Moreover, the CECs of the zeolites synthesized at 180 C (178–200 cmol kg^{-1}) were approximately three times higher than those of their counterparts synthesized at 100 C (46–57 cmol kg^{-1}). Despite using the same aging process to synthesize the zeolites, the CEC of the zeolites increased with increasing hydrothermal temperature. The CEC of the zeolite P synthesized at 180 °C is similar to those reported previously (Table S2) [31–34]. The significantly high CEC of the zeolites synthesized at 180 °C indicates their potential effectiveness in fields such as pollutant removal and water softening.

Table 4 lists the BET specific surface areas of the raw materials and synthesized zeolites; those of the zeolites synthesized at 100 and 180 C were 30–72 m^2 g^{-1} and 72–87 m^2 g^{-1}, respectively. The BET specific surface

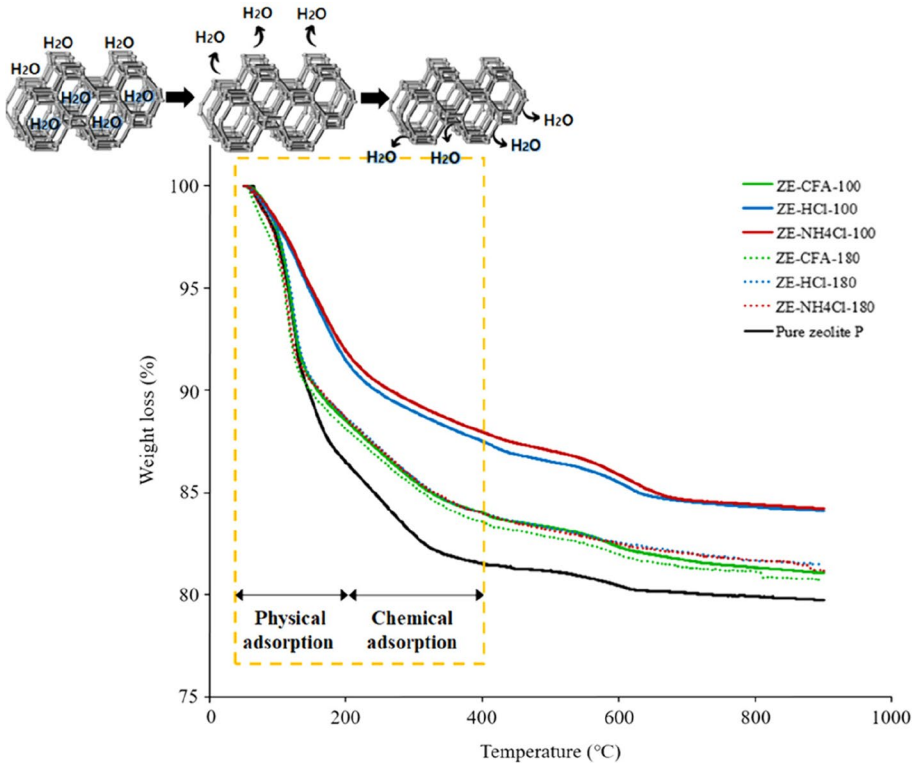

Fig. 3 TGA results of pure zeolite-P and the zeolites synthesized at 100 and 180 C

Table 2 Conversion efficiencies of zeolites synthesized using CFA and residual waste at 100 and 180 C

Material	Conversion efficiency (%)	
	100 C[a]	180 C[a]
ZE-CFA	84	89
ZE-HCl	67	87
ZE-NH_4Cl	65	87

[a] Hydrothermal reaction temperature

Table 3 CECs of the raw materials and synthesized zeolites

CEC (cmol kg^{-1})					
Raw material		Synthesized zeolite			
		100 C[a]		180 C[a]	
CFA	4.8	ZE-CFA-100	57	ZE-CFA-180	178
RW-HCl	5.3	ZE-HCl-100	46	ZE HCl-180	189
RW-NH_4Cl	5.1	ZE-NH_4Cl-100	46	ZE-NH_4Cl-180	200

[a] Hydrothermal reaction temperature

area of the zeolites increased with increasing hydrothermal temperature, similar to the CEC–temperature trend. The BET specific surface areas of the zeolites

Table 4 BET specific surface areas of the raw materials and synthesized zeolites

BET specific surface area (m^2 g^{-1})					
Raw material		Synthesized zeolite			
		100 °C[a]		180 °C[a]	
CFA	3.3	ZE-CFA-100	63	ZE-CFA-180	87
RW-HCl	6.0	ZE-HCl-100	72	ZE HCl-180	73
RW-NH_4Cl	4.6	ZE-NH_4Cl-100	30	ZE-NH_4Cl-180	72

[a] Hydrothermal reaction temperature

synthesized at 180 C (72–87 m^2 g^{-1}) were 12–26 times higher than those of the residual waste and CFA. These results are consistent with the surface characteristics observed through FE-SEM (Fig. 2) in terms of the surface-related differences between the smooth raw materials (residual waste and CFA) and the pore-rich and pointed synthetic zeolites. The specific surface areas of the zeolite P synthesized using residual waste and CFA were similar to or higher than those previously reported. For instance, in previous studies, the BET specific surface area of zeolite P synthesized using CFA via hydrothermal curing and aging is 19–88 m^2 g^{-1} (Table S3) [19, 20, 30, 32–35].

4 Conclusions

In this study, zeolite P was hydrothermally synthesized at 100 and 180 C using the residual waste from indirect carbonation without adding Si or Al. The zeolites hydrothermally synthesized at 180 C had higher CECs and larger specific surface areas than those of their counterparts synthesized at 100 C. Moreover, the CECs of the zeolites synthesized at 180 C (189–200 cmol kg^{-1}) were 36–39 times higher than those of the residual waste, while their BET specific surface areas (72–73 m^2 g^{-1}) were 12–16 times higher. The conversion efficiency of the zeolites synthesized at 180 C was remarkably high (87%), emphasizing the suitability of the residual waste as a material for zeolite synthesis. This approach on utilizing residual waste offers several advantages such as mitigating the disposal of substantial waste in landfills, which can lead to significant environmental and financial benefits. Additionally, materials with superior ion exchange and adsorption properties can be obtained through residual-waste-based zeolite synthesis. The zeolite-P hydrothermally synthesized using indirect-carbonation-derived residual waste could be used to remove pollutants, including heavy metals, ammonium ions, and toxic and radioactive waste species; extract potassium from seawater; and soften water. The use of residual waste from indirect carbonation can open new horizons for enabling the economical synthesis of zeolites, being promising for use in many applications and fields. Future work will involve extensive research on the production of calcium carbonate through indirect carbonation, while synthesizing zeolite using the residual waste generated during this process. An economic assessment of the entire process will be also conducted together with quantitative determination of the CO_2 stored and energy consumed.

Supplementary Information

The online version contains supplementary material available at https://doi.org/10.1186/s42834-023-00206-6.

Additional file 1: Table S1. Weight loss (%) of synthesized zeolites at 40–400 °C. **Table S2.** Cation-exchange capacities (CECs) of previously reported zeolites. **Table S3.** BET specific surface areas of previously reported zeolites.

Authors' contributions

Seonmi Shin: Conceptualization, Methodology, Investigation, Writing – original draft. Myoung-Jin Kim: Writing – review & editing, Validation, Supervision, Funding acquisition.

Funding

This work was supported by the National Research Foundation (NRF) of Korea grant funded by the Korean government (NRF-2021R1A2C2009914). This research was supported by Korea Institute of Marine Science & Technology Promotion (KIMST) funded by the Ministry of Oceans and Fisheries (20220149).

Availability of data and materials

Not applicable.

Declarations

Competing interests

The authors declare that they have no known competing financial interests or personal relationships that could have appeared to influence the work reported in this paper.

Received: 13 June 2023 Accepted: 26 December 2023
Published online: 02 January 2024

References

1. Yadav VK, Choudhary N, Tirth V, Kalasariya H, Gnanamoorthy G, Algahtani A, et al. A short review on the utilization of incense sticks ash as an emerging and overlooked material for the synthesis of zeolites. Crystals. 2021;11:1255.
2. Szerement J, Szatanik-Kloc A, Jarosz R, Bajda T, Mierzwa-Hersztek M. Contemporary applications of natural and synthetic zeolites from fly ash in agriculture and environmental protection. J Clean Prod. 2021;311:127461.
3. Karmen M, Anamarija F. Introductory chapter: Zeolites - From discovery to new applications on the global market. In: Karmen M, Anamarija F, editors. Zeolites - New Challenges. Rijeka: IntechOpen; 2020, p. 1–10.
4. Langauer D, Cablik V, Hredzak S, Zubrik A, Matik M, Dankova Z. Preparation of synthetic zeolites from coal fly ash by hydrothermal synthesis. Materials. 2021;14:1267.
5. Samal S. Utilization of red mud as a source for metal ions—A review. Materials. 2021;14:2211.
6. Sanna A, Uibu M, Caramanna G, Kuusik R, Maroto-Valer MM. A review of mineral carbonation technologies to sequester CO_2. Chem Soc Rev. 2014;43:8049–80.
7. Azdarpour A, Asadullah M, Mohammadian E, Hamidi H, Junin R, Karaei MA. A review on carbon dioxide mineral carbonation through pH-swing process. Chem Eng J. 2015;279:615–30.
8. Woodall CM, McQueen N, Pilorge H, Wilcox J. Utilization of mineral carbonation products: current state and potential. Greenh Gases. 2019;9:1096–113.
9. Bandura L, Woszuk A, Kołodynska D, Franus W. Application of mineral sorbents for removal of petroleum substances: A review. Minerals. 2017;7:37.
10. Woszuk A, Zofka A, Bandura L, Franus W. Effect of zeolite properties on asphalt foaming. Constr Build Mater. 2017;139:247–55.
11. Ho HJ, Iizuka A, Shibata E, Ojumu T. Circular indirect carbonation of coal fly ash for carbon dioxide capture and utilization. J Environ Chem Eng. 2022;10:108269.
12. Blissett RS, Rowson NA. A review of the multi-component utilisation of coal fly ash. Fuel. 2012;97:1–23.
13. Khaleque A, Alam MM, Hoque M, Mondal S, Haider JB, Xu B, et al. Zeolite synthesis from low-cost materials and environmental applications: A review. Environ Adv. 2020;2:100019.
14. Tauanov Z, Azat S, Baibatyrova A. A mini-review on coal fly ash properties, utilization and synthesis of zeolites. Int J Coal Prep Util. 2022;42:1968–90.
15. Majchrzak-Kucęba I. A simple thermogravimetric method for the evaluation of the degree of fly ash conversion into zeolite material. J Porous Mat. 2013;20:407–15.
16. Kim MJ, Pak SY, Kim D, Jung S. Optimum conditions for extracting Ca from CKD to store CO_2 through indirect mineral carbonation. KSCE J Civ Eng. 2017;21:629–35.
17. Kim D, Kim MJ. Calcium extraction from paper sludge ash using various solvents to store carbon dioxide. KSCE J Civ Eng. 2018;22:4799–805.
18. Kim MJ, Kim D. Maximization of CO_2 storage for various solvent types in indirect carbonation using paper sludge ash. Environ Sci Pollut R. 2018;25:30101–9.
19. Aldahri T, Behin J, Kazemian H, Rohani S. Synthesis of zeolite Na-P from coal fly ash by thermo-sonochemical treatment. Fuel. 2016;182:494–501.

20. Liu Y, Yan C, Zhao J, Zhang Z, Wang H, Zhou S, et al. Synthesis of zeolite P1 from fly ash under solvent-free conditions for ammonium removal from water. J Clean Prod. 2018;202:11–22.
21. Wang P, Sun Q, Zhang Y, Cao J. Hydrothermal synthesis of magnetic zeolite P from fly ash and its properties. Mater Res Express. 2020;7:016104.
22. Zhao XS, Lu GQ, Zhu HY. Effects of ageing and seeding on the formation of zeolite Y from coal fly ash. J Porous Mat. 1997;4:245–51.
23. Anuwattana R, Khummongkol P. Conventional hydrothermal synthesis of Na-A zeolite from cupola slag and aluminum sludge. J Hazard Mater. 2009;166:227–32.
24. Kamimura Y, Itabashi K, Okubo T. Seed-assisted, OSDA-free synthesis of MTW-type zeolite and "Green MTW" from sodium aluminosilicate gel systems. Micropor Mesopor Mat. 2012;147:149–56.
25. Murayama N, Yamamoto H, Shibata J. Mechanism of zeolite synthesis from coal fly ash by alkali hydrothermal reaction. Int J Miner Process. 2002;64:1–17.
26. Munthali MW, Elsheikh MA, Johan E, Matsue N. Proton adsorption selectivity of zeolites in aqueous media: Effect of Si/Al ratio of zeolites. Molecules. 2014;19:20468–81.
27. Huo Z, Xu X, Lu Z, Song J, He M, Li Z, et al. Synthesis of zeolite NaP with controllable morphologies. Micropor Mesopor Mat. 2012;158:137–40.
28. Musyoka NM, Petrik LF, Hums E, Kuhnt A, Schwieger W. Thermal stability studies of zeolites A and X synthesized from South African coal fly ash. Res Chem Intermediat. 2015;41:575–82.
29. Apiratikul R, Pavasant P. Sorption of Cu^{2+}, Cd^{2+}, and Pb^{2+} using modified zeolite from coal fly ash. Chem Eng J. 2008;144:245–58.
30. Izidoro JC, Fungaro DA, dos Santos FS, Wang S. Characteristics of Brazilian coal fly ashes and their synthesized zeolites. Fuel Process Technol. 2012;97:38–44.
31. Johan E, Yamada T, Munthali MW, Kabwadza-Corner P, Aono H, Matsue N. Natural zeolites as potential materials for decontamination of radioactive cesium. Procedia Environ Sci. 2015;28:52–6.
32. Goscianska J, Ptaszkowska-Koniarz M, Frankowski M, Franus M, Panek R, Franus W. Removal of phosphate from water by lanthanum-modified zeolites obtained from fly ash. J Colloid Interf Sci. 2018;513:72–81.
33. Aldahri T, Behin J, Kazemian H, Rohani S. Effect of microwave irradiation on crystal growth of zeolitized coal fly ash with different solid/liquid ratios. Adv Powder Technol. 2017;28:2865–74.
34. Qiu X, Liu Y, Li D, Yan C. Preparation of NaP zeolite block from fly ash-based geopolymer via in situ hydrothermal method. J Porous Mat. 2015;22:291–9.
35. Franus W, Wdowin M, Franus M. Synthesis and characterization of zeolites prepared from industrial fly ash. Environ Monit Assess. 2014;186:5721–9.

Publisher's Note